International Current Journal of Engineering and Science (ICJES)
Volume 4, Issue 11, pp 36-41, November-2025
ISSN (Online): 2583-7257
Article DOI: https://doi.org/10.47001/ICJES/2025.411007

Gearbox Fault Identification through Cyclostationary Analysis of Vibration Signals

[1]Achmad Widodo, [2]*Ismoyo Haryanto, [3]Mahendra Haryo, [4]Toni Prahasto, [5]Ojo Kurdi

[1,2,4,5]Department of Mechanical Engineering, Universitas Diponegoro, Semarang, Indonesia
[3]Undergraduate Program, Department of Mechanical Engineering, Universitas Diponegoro, Semarang, Indonesia
*Corresponding Author's E-mail: ismoyo2001@yahoo.de

Abstract - **Gearboxes are critical components that ensure the operational continuity of industrial machinery. Gearbox failures may arise from material defects, design errors, manufacturing inconsistencies, surface wear, excessive torque loading, and fatigue. Among these, the most frequently observed failures are associated with gear damage, including abrasive wear, cracking, and tooth breakage. Consequently, reliable diagnostic methods are required, and vibration signal analysis using cyclostationary techniques has emerged as a promising approach. A cyclostationary process is a specific class of non-stationary process characterized by periodic variations in its statistical moments. This study examines the condition monitoring of a Suzlon wind turbine using secondary data consisting of 11 samples for each operating condition: normal and faulty. The FFT spectrum analysis indicates average frequencies of the GNF, 1×GMF, and 2×GMF at 473.4 Hz, 925.3 Hz, and 1851.2 Hz, respectively, accompanied by multiple sidebands. The spectral correlation density (SCD) results show corresponding average frequencies of 470.4 Hz, 920.7 Hz, and 1841.0 Hz, also exhibiting sideband structures. Based on the diagnostic outcomes, the gearbox is strongly indicated to exhibit three fault types: wear, eccentricity with backlash, and cracking.**

Keywords: Machine diagnostics; Gearbox; Cyclostationary; Vibration; Spectral correlation density.

I. INTRODUCTION

In the era of Industry 4.0, computer and information technologies have been extensively applied in maintenance and repair activities across strategic industries such as oil and gas, power generation, transportation, and defense. These industries place significant emphasis on maintaining the operational continuity of critical machine components. Consequently, effective diagnostic methods are required to detect component degradation and accurately estimate the remaining useful life of machinery. Among machine elements, gearboxes are particularly sensitive to high vibration levels and are therefore of considerable interest for condition monitoring applications [1,2].

A gearbox consists of multiple gear stages designed to deliver the desired power transmission characteristics. Its primary functions include modifying rotational speed and torque. Various gearbox configurations exist to enable machinery to increase torque and power from low-speed input to high-speed output. Gearboxes offer several advantages, including the ability to achieve high rotational speeds for power generation and to deliver high torque, while also being lightweight and compact for installation in constrained environments [3].

Gearbox failures may arise from material defects, design inaccuracies, manufacturing errors, surface wear, excessive torque loading, and fatigue. The most frequently reported failures are associated with gear damage, including abrasive wear, cracking, and tooth breakage [4]. Such failures can cause increased temperatures in the bearings and lubricating oil, which serve as indicators of developing faults.

This study focuses on the analysis of vibration signals using cyclostationary techniques for gearbox fault diagnosis in wind turbine applications [5-8]. The dataset consists of secondary vibration measurements from a wind turbine gearbox, recorded by Bechhoefer [9]. Each sample is analyzed using cyclostationary methods to assess the gearbox condition.

II. METHOD AND MATERIALS

The research procedure employed in this study is illustrated in Fig. 1. Following an initial literature review, the first stage involves data acquisition. The dataset was obtained from the work of Bechhoefer, who conducted condition monitoring of gear components in a wind turbine gearbox. The acquired signals were initially processed using the Fast Fourier Transform (FFT) to obtain the vibration spectrum in the frequency domain. Subsequently, the spectral correlation density (SCD) method was applied to analyze the cyclostationary characteristics of the signals, as described in [5-7].

Volume 4, Issue 11, pp 36-41, November-2025
ISSN (Online): 2583-7257
Article DOI: https://doi.org/10.47001/ICJES/2025.411007

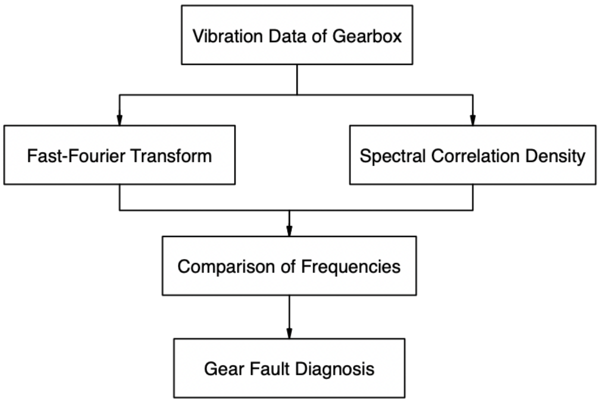

Figure 1: The proposed method

Fast Fourier Transform (FFT)

2.1 Cyclostationary Process

Cyclostationary processes represent a specific class of non-stationary processes characterized by periodic variations in their statistical moments [10-11]. Two principal approaches are used to analyze these processes: the probabilistic and non-probabilistic approaches.

2.1.1 Probabilistic Approach

The probabilistic formulation is based on the time-averaged behavior of the signal *x(t)* and provides analytical convenience for signal manipulation, as noted in [12]. First-order cyclostationarity is defined by periodicity in the probability density function and the mean value, as shown in Eqs. (2)–(3).

$$f_x\big(x(t)\big) = f_x(x(t+nT)) \qquad (2)$$

$$E\{x(t)\} = E\{(t+nT)\} \qquad (3)$$

Where $f_x(x)$ is probability density function, n is integer, $x(t)$ is time domain signal, $E(x)$ is expectation function and T is period of the function.

Second-order cyclostationarity is defined by the periodicity of the autocorrelation function, expressed in Eq. (4).

$$R_x(t,\tau) = E\{x(t+nT)x(t+nT-\tau)\} \qquad (4)$$

$$= R_x(t+T,\tau)$$

Where,

$R(t,\tau)$: autocorrealtion function

τ : time delay between two signals

t : real time, i.e., the initial time at which the autocorrelation is computed

When expanded using a Fourier series, the cyclic autocorrelation takes the form shown in Eqs. (5)–(6)

$$R_x(\mathrm{t},\tau) = \sum_\alpha R_x^\alpha(\tau)e^{j2\pi\alpha t} \qquad (5)$$

$$R_x^\alpha(\tau) = E\{R_x\,(t,\tau)e^{-j2\pi\alpha t}\}$$

$$= E\{x\left(t+\tfrac{\tau}{2}\right)x*\left(t-\tfrac{\tau}{2}\right)e^{-j2\pi\alpha t} \qquad (6)$$

Volume 4, Issue 11, pp 36-41, November-2025
ISSN (Online): 2583-7257
Article DOI: https://doi.org/10.47001/ICJES/2025.411007

Where $R_x^\alpha(\tau)$ denotes the cyclic autocorrelation coefficient and α=1/T is the cyclic frequency.

First-order cyclostationary processes exhibit a mean that varies periodically with period T, whereas first-order stationary processes exhibit constant mean values. Second-order cyclostationarity forms the basis for the spectral correlation density (SCD), which provides a frequency-domain representation of cyclostationary behavior.

2.1.2 Non-Probabilistic Approach

The non-probabilistic approach relies on time averaging and is suitable for practical signal-processing applications [2]. This formulation is expressed in Eqs. (7)–(8), followed by a Fourier-series representation of the cyclic autocorrelation.

$$Rx(\mathrm{t},\tau) = \lim_{N\to\infty} \sum_{n=-N}^{N} x\left(t + nT + \frac{\tau}{2}\right) x * \left(t + nT - \frac{\tau}{2}\right) \quad (7)$$

$$R_x^\alpha(\tau) = \lim_{T\to\infty} \int_{-T/2}^{T/2} \left(t + nT + \frac{\tau}{2}\right) x * \left(t + nT - \frac{\tau}{2}\right) e^{-j2\pi\alpha t}\,\mathrm{dt} \quad (8)$$

The spectral correlation density (SCD) is the principal tool used to reveal cyclostationary features. It is defined as the Fourier transform of the cyclic autocorrelation function, as shown in Eq. (9). The SCD depends on both the spectral frequency f and the cyclic frequency α. For α=0, the SCD reduces to the power spectral density of the signal; for α≠0, the SCD corresponds to the cross-spectral density between the signal and a frequency-shifted version of itself.

$$S_x^\alpha(f) = \int_{-\infty}^{+\infty} R_x^\alpha\,(\tau) e^{-j2\pi f\tau}\, d\tau \quad (9)$$

2.1.3 Cyclostationary Signal Model for Gearbox Vibrations

The primary source of excitation in the vibration of a spiral gear pair arises from the gear-meshing force. For gears operating at constant load and constant rotational speed, with one gear having z teeth and rotating at f_r , the meshing frequency is given by $f_m = zf_r$. The resulting mesh vibration x(t) may be represented as a harmonic series, as given in Eq. (10) [13-15].

$$\boldsymbol{x}(\mathbf{t}) = \sum_{n=0}^{N} \boldsymbol{X_n cos(2\pi n f_m t + \emptyset_n)} \quad (10)$$

Where,

- x(t) :Gear-meshing vibration signal
- f_m : Gear-meshing frequency
- X_n : Amplitude of the n-th component
- N : Index of the n-th meshing harmonic
- ϕ_n : Phase angle of the n-th mesh harmonic
- f_r : Rotational frequency

Variations in this vibration signal result from amplitude and phase modulation, yielding the modulated signal $y(t)$ in Eq. (11), where a_n(t) and b_n(t) denote amplitude and phase modulation functions. Because these modulation functions are periodic with the shaft rotational frequency, they may be expressed using Fourier-series expansions, as shown in Eq. (12).

$$\boldsymbol{y}(\mathbf{t}) = \sum_{n=0}^{N} \boldsymbol{X_n[1 + a_n(t)]cos[2\pi n f_m t + \emptyset_n + b_n(t)]} \quad (11)$$

$$\boldsymbol{a_n}(\mathbf{t}) = \sum_{m=0}^{M} \boldsymbol{A_{nm} cos(2\pi m f_r t + \alpha_{nm})}$$

$$\boldsymbol{b_m}(\mathbf{t}) = \sum_{m=0}^{M} \boldsymbol{B_{nm} cos(2\pi m f_r t + \beta_{nm})} \quad (12)$$

International Current Journal of Engineering and Science (ICJES)
Volume 4, Issue 11, pp 36-41, November-2025
ISSN (Online): 2583-7257
Article DOI: https://doi.org/10.47001/ICJES/2025.411007

III. RESULTS AND DISCUSSION

Data processing using the Fast Fourier Transform (FFT) and the Spectral Correlation Density (SCD) feature yields vibration frequency plots that present several diagnostic indicators for gearbox fault analysis. The primary indicators include the 1× revolutions per minute (RPM), 2× RPM, the 1× gear natural frequency (GNF), the 1× gear mesh frequency (GMF), the 2× GMF, as well as the sidebands associated with both GNF and GMF.

The results of the FFT-based vibration analysis are presented as follows. The vibration frequency plot under normal operating conditions is shown in Fig. 2.a, whereas Fig. 2.b depicts the vibration frequency plot corresponding to the faulty condition.

The analysis of the vibration signals using both the Fast Fourier Transform (FFT) and the SCD reveals several important diagnostic characteristics associated with the health condition of the gearbox. As observed in the plots provided in the accompanying document, the vibration spectra exhibit prominent signatures at the gear natural frequency (GNF), the gear mesh frequency (GMF), and its harmonics, along with multiple sidebands spaced approximately at the rotational frequency. These signatures form the basis of the fault diagnosis.

a) Interpretation of FFT and SCD characteristics

The SCD results demonstrate clearly defined cyclic spectral peaks at the GNF, 1×GMF, and 2×GMF, as well as sidebands whose spacing corresponds to the shaft rotational frequency. This structure is indicative of amplitude or phase modulation resulting from gear wear, eccentricity, backlash, or tooth cracking. Compared with FFT, the SCD representations highlight the cyclostationary components more distinctly, resulting in sharper and more interpretable peaks. Minor frequency deviations between FFT and SCD measurements (e.g., for the GNF) are expected because SCD enhances cyclically coherent components, whereas FFT aggregates all spectral energy including noise.

The resulting vibration frequency plots obtained using the spectral correlation density (SCD) feature under normal operating conditions are presented in Fig. 3. Meanwhile, Fig. 4 and Fig. 5 illustrate the vibration frequency plot generated using the SCD feature under normal and the faulty condition, respectively.

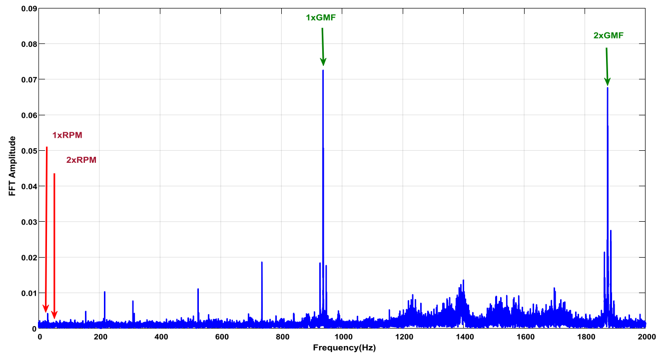

(a)

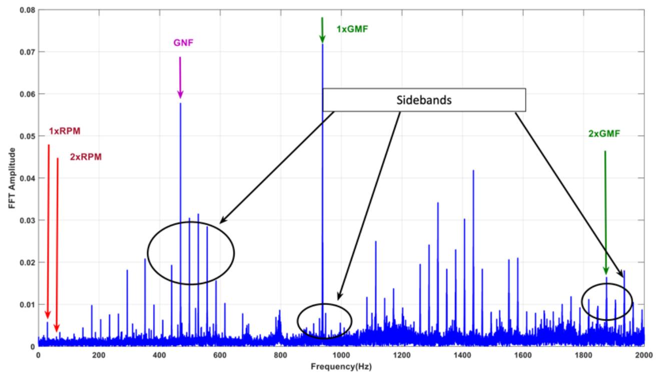

(b)

Figure 2: Signal frequency domain: (a) normal condition; (b) faulty condition

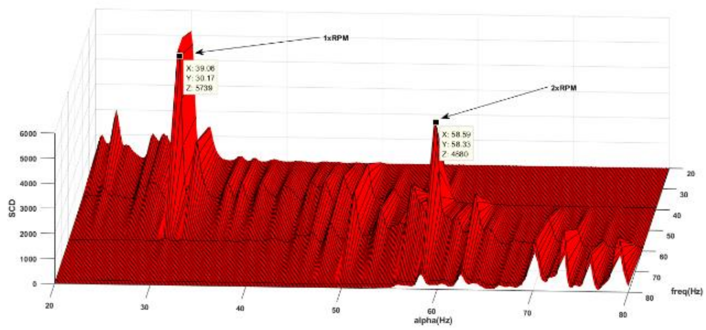

Figure 3: SCD results for normal conditions 1xRPM and 2xRPM

b) Diagnostic indicators derived from SCD

The differences between the normal and faulty gearbox samples are consistent with typical fault mechanisms. Normal samples displays lower 1×RPM amplitude and do not exhibit significant GNF components or pronounced sideband structures. Meanwhile, faulty samples show consistent presence of the GNF around 460–490 Hz; pronounced sidebands around GNF, GMF, and 2×GMF spaced at approximately ±30 Hz (rotational frequency); and elevated 1×RPM amplitudes. These features collectively indicate wear, eccentricity/backlash, and crack-related faults.

International Current Journal of Engineering and Science (ICJES)
Volume 4, Issue 11, pp 36-41, November-2025
ISSN (Online): 2583-7257
Article DOI: https://doi.org/10.47001/ICJES/2025.411007

In particular, wear is suggested by the appearance of GNF and surrounding sidebands, accompanied by moderate sidebands around GMF. Eccentricity/backlash produces stronger and more numerous sidebands around GMF. Cracked tooth faults exhibit increased 1×RPM amplitude, GNF components, and dominant sidebands around GMF. These diagnostic indicators align with established criteria in the literature and provide a reliable basis for fault assessment.

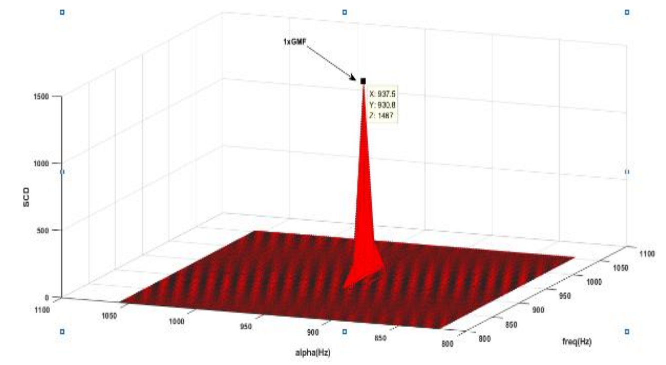

(a)

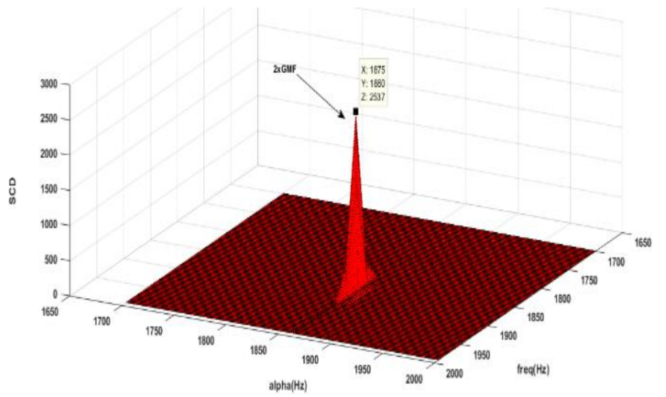

(b)

Figure 4: SCD results under normal conditions at (a) 1xGMF (b) 2xGMF

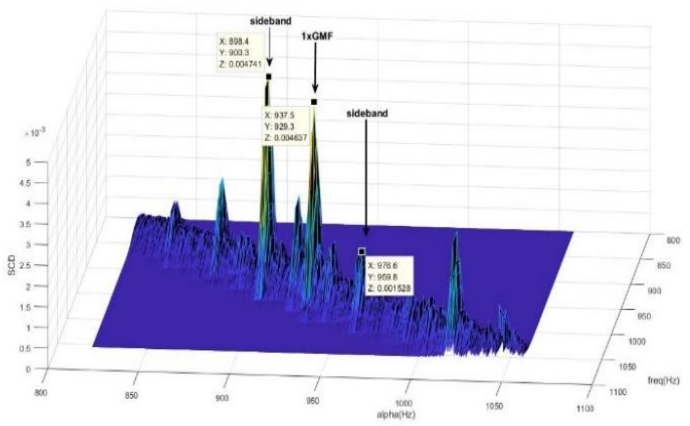

(a)

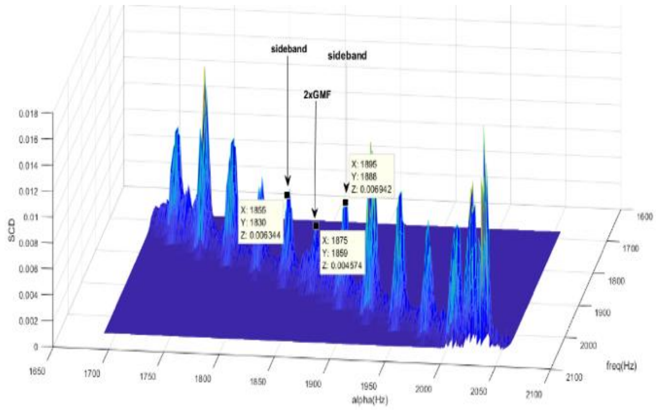

(b)

Figure 5: SCD results of damaged conditions at (a) 1xGMF (b) 2xGMF

IV. CONCLUSIONS

In this study, the cyclostationary method using the Spectral Correlation Density (SCD) function proved to be highly effective for diagnosing gearbox faults. The three-dimensional bi-frequency representation produced by SCD enabled clear identification of frequency peaks and sidebands that are not easily distinguishable using conventional FFT analysis. Faulty gearbox samples consistently exhibited an increased rotational frequency (1×RPM), the appearance of the Gear Natural Frequency (GNF) at 460–490 Hz, and high-amplitude sidebands spaced at ±30 Hz around GNF, 1×GMF, and 2×GMF. Based on these features, three primary fault types were identified across the samples: wear, eccentricity/backlash, and tooth cracking.

Although the SCD method provides enhanced sensitivity to modulated and periodic vibration components, several limitations remain:

1. The computational cost of SCD is significantly higher compared with FFT-based techniques.
2. The accuracy of SCD results depends on the quality and length of vibration data, which may introduce variability in field applications.
3. The method assumes a relatively steady rotational speed, which may not hold in systems with large speed fluctuations.

To improve diagnostic reliability, the following recommendations are proposed:

1. Combine SCD analysis with time–frequency methods (e.g., CWT or STFT) to enhance robustness under variable-speed conditions.

Volume 4, Issue 11, pp 36-41, November-2025
ISSN (Online): 2583-7257
Article DOI: https://doi.org/10.47001/ICJES/2025.411007

2. Incorporate automated feature extraction and classification using machine learning to reduce operator dependency.
3. Improve data acquisition resolution to better capture sidebands with small amplitude differences.

REFERENCES

[1] T. Hasegawa et al., "Adaptive training of vibration-based anomaly detector for wind turbine condition monitoring," *Waseda University, Japan,* 2017.

[2] F. Liao, C. Sun, and B. Tang, "Wind turbine gear fault detection based on improved cyclostationary analysis with adaptive time–frequency reassignment," *Renewable Energy*, vol. 195, pp. 245–258, 2023.

[3] L. Hossain, A. Abu-Siada, and S. M. Muyeen, "Methods for advanced wind turbine condition monitoring and early diagnosis: A literature review," *Curtin Univ., Australia,* 2018.

[4] D. J. Wulpi, Understanding How Components Fail, *2nd ed. Ohio, USA: ASM International*, 1999.

[5] J. Antoni, "Cyclic spectral analysis in practice," *Mechanical Systems and Signal Processing*, vol. 21, no. 2, pp. 597–630, 2007.

[6] F. Liao, C. Sun, and B. Tang, "Wind turbine gear fault detection based on improved cyclostationary analysis with adaptive time–frequency reassignment," *Renewable Energy*, vol. 195, pp. 245–258, 2023.

[7] M. H. Zhang and T. Y. Lee, "Cyclostationary feature-enhanced transformers for intelligent gearbox fault detection," *IEEE Transactions on Instrumentation and Measurement*, vol. 73, pp. 1–12, 2024.

[8] K. R. Singh and P. K. Kankar, "Gearbox fault diagnosis using enhanced spectral kurtosis and CNN-based classification," *Mechanical Systems and Signal Processing*, vol. 172, p. 109063, 2022.

[9] E. Bechhoefer, "High Speed Gear Dataset." Available: http://data-acoustics.com/measurements/gearfaults/gear-1/. Accessed: May 28, 2019.

[10] W. A. Gardner, Introduction to Random Processes with Applications to Signals and Systems. *New York, NY, USA: McGraw-Hill*, 1986.

[11] W. A. Gardner, A. Napolitano, and L. Paura, "Cyclostationarity: Half a century of research," *Signal Processing*, vol. 86, no. 4, pp. 639–697, 2006.

[12] P. Gidhar and C. Scheffer, Practical Machinery Vibration Analysis and Predictive Maintenance. *Oxford, UK: Elsevier*, 2004.

[13] P. D. McFadden, "Detecting fatigue cracks in gears by amplitude and phase demodulation of the meshing vibration," *Journal of Vibration, Acoustics, Stress, and Reliability in Design*, vol. 108, pp. 165–170, 1986.

[14] J. Martínez, F. Pineda, and R. Ruiz, "Vibration-based predictive maintenance of wind turbine gearboxes using digital twin models and cyclostationary analysis," *Energy Reports*, vol. 10, pp. 188–199, 2024.

[15] S. S. Rao and H. Jiang, "Advanced gear health monitoring using 3D spectral correlation and machine learning," *IEEE Access*, vol. 11, pp. 112345–112358, 2023.

Citation of this Article:

Achmad Widodo, Ismoyo Haryanto, Mahendra Haryo, Toni Prahasto, & Ojo Kurdi. (2025). Gearbox Fault Identification through Cyclostationary Analysis of Vibration Signals. *International Current Journal of Engineering and Science (ICJES)*, 4(11), 36-41. Article DOI: https://doi.org/10.47001/ICJES/2025.411007

****